Significance of quantum size effects in the conductivity of granular Pd_xC_{1-x} films

A. Carl,* G. Dumpich, and E. F. Wassermann
Tieftemperaturphysik, Universität Duisburg, 47057 Duisburg, Federal Republic of Germany
(Received 2 August 1993)

We report on structural and electrical properties of thin granular Pd_xC_{1-x} films with palladium (Pd) metal volume fractions $0.3 < x < 0.34$, approaching the percolation threshold ($x_p = 0.3$) from the metallic side. As revealed from transmission-electron microscopy, granular Pd_xC_{1-x} films consist of small spherical Pd clusters with mean diameters Φ ranging between 3 nm $< \Phi <$ 4 nm, embedded in an amorphous carbon (C) matrix. The Pd clusters are only weakly coupled, forming an infinite percolative network within the amorphous-C matrix. The whole network is progressively disrupted with decreasing x. The overall conductivity behavior of the films is metallic, strongly influenced by electron localization and electron-electron interaction effects. The temperature dependence of the dc conductivity follows $\sigma(T) \propto T^{1/2}$ over a large range in temperature at elevated temperatures, similar to what is expected for three-dimensional (3D) *homogeneous* systems. However, below distinct low temperatures T_δ we observe characteristic deviations from the $\sigma(T) \propto T^{1/2}$ law towards a stronger than logarithmic temperature dependence of $\sigma(T)$, and a saturation of $\sigma(T)$ for $T \rightarrow 0$. This does not result from a dimensional (3D$\rightarrow$2D) crossover with respect to localization and electron-electron interaction, but is discussed as resulting from the influence of the granular film structure on electronic transport, since T_δ is for all films related to the mean cluster diameter Φ via $k_B T_\delta = [N(E_F)\Phi^3]^{-1}$. Here, $k_B T_\delta$ is the average energy level separation within the small metallic clusters due to quantum size effects (QSE). These are known to be of significance in the transport properties of insulating granular films. With this paper we propose that likewise QSE are of importance for granular metallic films.

I. INTRODUCTION

The electrical transport properties of granular thin films have been widely investigated for several decades.[1-12] A complete understanding of their physical nature, however, is still missing, especially for granular films within the transition region from metallic to insulating behavior. Here the main difficulty that prevents a comprehensive theoretical description is that the true relationship between conductivity and a particular film structure is not well known up to now.

Granular films are mostly prepared by coevaporation or cosputtering of two insoluble components, one of which is metallic and the other insulating, such as Ni-SiO_2, Pt-SiO_2, Au-Al_2O_3, or W-Al_2O_3.[3,4] Their structural properties are rather similar, and their physical properties strongly depend on the metal volume fraction x, which can be controlled experimentally by means of different evaporation rates during sample preparation. For metal volume fractions $x < x_p$, where x_p is the so-called percolation threshold, granular films are built up mostly from disconnected small (usually < 10 nm) metallic cluster with a rather narrow distribution of cluster diameters, embedded in an electrically insulating matrix. With increasing x, more and more clusters coagulate, forming cluster aggregates, until at a certain metal volume fraction $x = x_p$ an infinite, percolative network exists throughout the entire sample. Upon further increasing x, for $x > x_p$, granular films then consist of metallic clusters that are connected by metallic bottlenecks, the number and lateral size of which increase with increasing x.

Obviously, the electrical transport properties—which are related to *global* film disorder—are very different for films with various metal volume fractions x. For a granular system we may specify global disorder with respect to different length scales; (i) disorder on microscopic length scales (e.g., lattice imperfections within small metallic clusters), which can be expressed in terms of an elastic electron mean free path l_e and (ii) disorder an macroscopic length scales, related to the granular film structure, which may be specified through average values of cluster-size and cluster distance (being suitable parameters to describe the *connectivity* of the granular network in terms of percolation models). In the following we distinguish between three different regimes, $x > x_p$, $x < x_p$, and $x \approx x_p$, respectively, where disorder on microscopic and/or macroscopic length scales is of different relative importance with respect to the conductivity.

For films with $x \gg x_p$, for which the typical granular structure is rather less pronounced, only disorder on microscopic length scales dominates the conductivity σ, and the behavior is bulklike metallic.[7,9,13,14] At slightly lower metal volume fraction, any structural inhomogeneities can be regarded as contributing in a global manner to the disorder on microscopic length scales, which may be expressed in terms of both a reduced *effective* electron mean free path l_e and diffusion coefficient $D = v_F l_e/3$ of the conduction electrons, respectively, with v_F the Fermi velocity. Any granular system with a large metal volume fraction can therefore be regarded as being quasihomogeneous. The electron diffusion averages over the structural inhomogeneities.[13,14] On the other hand, the reduction of electronic diffusion leads to important quan-

tummechanical corrections to the classical "Boltzmann" conductivity at low temperatures, resulting from both "weak" electron localization (WL) (Ref. 15) and enhanced electron electron interaction (EEI).[16] This has been confirmed experimentally for both two-dimensional (2D) (Refs. 7,14, and 17) as well as 3D (Refs. 13 and 18) granular films. In 2D systems logarithmic corrections, $\delta\sigma \propto \ln(T)$, and 3D systems square-root corrections, $\delta\sigma \propto T^{1/2}$, have been observed in the low-temperature conductivity behavior. Both dependencies are confirmed theoretically[15,16] as well as experimentally on structurally homogeneous films.[19,20]

On the other hand, films with $x \ll x_p$ reveal typical granular structure, with isolated, small metallic clusters embedded in an amorphous insulating matrix. Here disorder on macroscopic length scales should play the more important role with respect to electronic transport, since the conductivity clearly depends on the particular arrangement of clusters within the sample. Several experimental investigations of different granular systems have revealed a unique temperature dependence of the conductivity σ, in the form

$$\sigma(T)=\sigma_0 \exp\left[-\left[\frac{T_0}{T}\right]^{1/2}\right], \quad (1)$$

where σ_0, $T_0=\text{const.}$[21-24] Up to now the physical origin of this temperature dependence of σ is discussed controversially in the literature within different theoretical concepts.[3,25-32] Most experimental results are analyzed within a theoretical model by Abeles *et al.*,[3] where the electronic transport is explained as resulting from thermally activated or field-induced tunneling of electrons between isolated nearest-neighbor clusters. Also, variable-range-hopping (VRH) transport in the presence of a Coulomb gap in the electronic density of states (DOS) near the Fermi energy E_F has been proposed as an appropriate conductivity mechanism for granular films with $x < x_p$,[27,29] in close analogy to a theory by Efros and Shklovskii[33] for amorphous semiconductors. It is only necessary for granular systems to scale up the relevant lengths of electronic hopping transport from microscopic to mesoscopic scales.[27] Since granular films with $x < x_p$ are composed of small isolated clusters, quantum size effects (QSE) have been proposed to be of importance for the conductivity behavior at low temperatures.[25-27] Here we are not concerned in QSE resulting in resistance oscillations versus film thickness, if the thickness of a thin film is comparable with the Fermi wavelength of the conduction electrons.[34] It is well known[25] that in small spherical particles with diameter Φ, QSE lead to discrete energy levels with separation δ given by[36]

$$\delta=\frac{1}{N(E_F)\Phi^3}, \quad (2)$$

where $N(E_F)$ is the density of states (DOS) at the Fermi energy E_F. Thus, for temperatures smaller than a characteristic temperature $T_\delta=\delta/k_B$, QSE are expected to cause modifications in the physical properties of small particles. For $T > \delta/k_B$, when the level separation is smeared out with temperature, the particle should behave bulklike.[36,37]

So far QSE have not been considered to be of relevance for the electrical transport of *metallic* granular films ($x > x_p$). Based on our experimental results for the conductivity behavior of granular Pd_xC_{1-x} films with $x \approx x_p$, we will show that below $T \approx 15$ K QSE can explain the low-temperature conductivity observed.

II. EXPERIMENT

Granular Pd_xC_{1-x} films with a metal volume fraction $0.1 < x < 1$ and thicknesses $t < 32$ nm have been prepared by coevaporation of high-purity palladium (99.999%, < 1-ppm magnetic impurity concentration) and high-purity carbon (< 0.1 at. % impurity concentration) simultaneously onto different substrates at room temperature in an UHV system ($p_0 < 10^{-7}$ Pa). Palladium (Pd) is evaporated by means of an electron-beam source and carbon (C) is sublimated from a resistively heated carbon rod. By using different evaporation rates for Pd and C, we are able to prepare Pd_xC_{1-x} films with various compositions and thicknesses. The deposition of Pd and C is independently monitored by two separate quartz-oscillator balances, which are calibrated by optical interferometry (Tolansky). From this we obtain the total film thickness $t=t_{Pd}+t_C$ and metal volume fraction $x=t_{Pd}/(t_{Pd}+t_C)$ with an accuracy of $\Delta x=\pm 5\times 10^{-3}$.

To reveal the relation between film structure and conductivity, in each run films with equal composition are simultaneously deposited onto NaCl and quartz-crystal substrates, respectively. The film on the cleaved NaCl substrate is investigated in a transmission-electron microscope (TEM), and the sample deposited onto the quartz crystal is used for resistance measurements. To yield equal condensation conditions for the films deposited onto the different substrates, both NaCl and quartz have been precoated with an amorphous carbon layer. The temperature dependence of the resistance is measured *in situ* between 3 and 300 K in a ^{4}He-gas-flow cryostate, using four-terminal dc technique (measuring currents 1–10 μA) with a resolution of $\Delta R/R \approx 10^{-5}$. Resistance contributions from the carbon sublayers are negligible, because absolute values are by orders of magnitude larger than those of the respective granular films. In addition, the magnetoresistance (MR) is measured *ex situ* in a ^{4}He-bath cryostate between 1.5 and 30 K within external magnetic fields perpendicular as well as parallel to the film plane up to $B=4.5$ T. Although the films are exposed to air during transfer, within the accuracy limits no difference was found in the temperature dependence of the resistance, due to a high stability of the films.

III. RESULTS

Figure 1 shows a typical electron micrograph of a Pd_xC_{1-x} films with $x=0.34$ close to the percolation threshold $x_p=0.3$ and thickness $t=21.2$ nm. The film consists of small Pd clusters (dark areas), forming an infinite percolative network within the amorphous C matrix (light areas). A closer look at the micrograph in Fig.

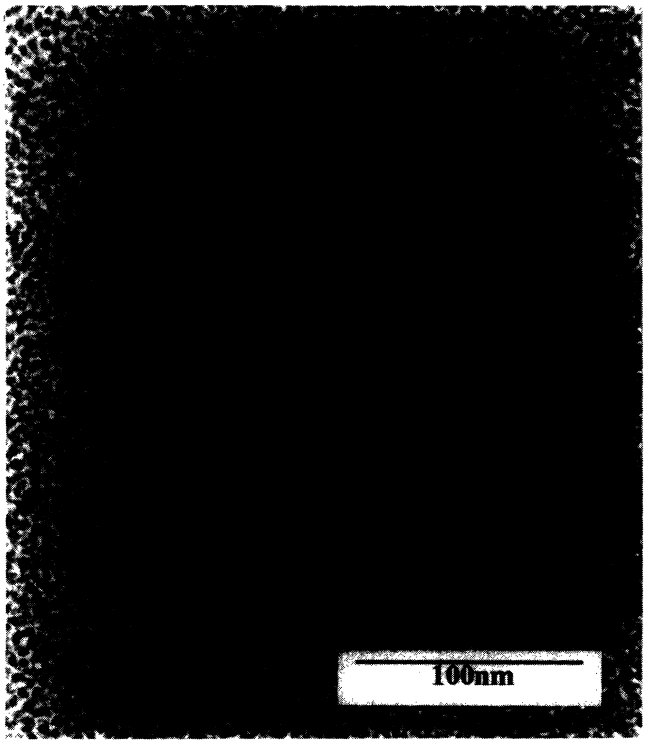

FIG. 1. Electron micrograph of a Pd_xC_{1-x} film with $x=0.34$ and $t=21.2$ nm.

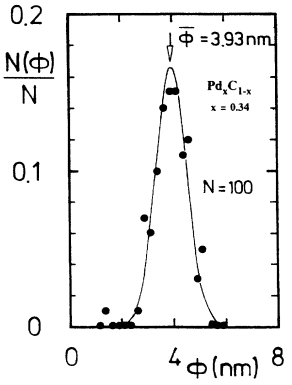

FIG. 2. Cluster-size distribution $N(\Phi)$ vs Φ, normalized to the total amount of clusters counted ($N=100$) for the Pd_1C_{1-x} film with $x=0.34$ shown in Fig. 1. The full dots are obtained experimentally by measuring cluster diameters with an accuracy of $\delta\Phi=0.05$ nm from TEM micrographs. The solid line represents a fit of a Gaussian distribution function to the data from which we obtain the mean cluster diameter $\Phi=3.93$ with standard deviation $\sigma_\Phi=\pm 0.6$ nm.

1 reveals that (i) most of the Pd clusters are weakly coupled by small bottlenecklike connections, and (ii) there are also completely isolated clusters. The morphology as shown in Fig. 1 is typical for all our films, and results from the immiscibility of C and Pd. The Pd clusters are crystalline, as revealed by electron diffraction. We always find fcc (111) fiber textures. The mean lattice constant $a=0.395$ nm is close to the bulk value $a=0.389$ nm for pure Pd, and independent of the carbon content. This confirms that the solubility of C in Pd is indeed unlikely.[38] The small lattice expansion of roughly 2% most probably results from an incorporation of small amounts of hydrogen during film deposition.[39]

In Fig. 2 we present the normalized cluster-size distribution $N(\Phi)/N$ for the Pd_xC_{1-x} film with $x=0.34$, shown in Fig. 1, where N is the total amount of clusters counted (typically $100<N<1000$), and $N(\Phi)$ the number of clusters with diameter Φ within an interval $\Delta\Phi=0.25$ nm. The values of $N(\Phi)$ (full dots) are obtained from the electron micrograph by measuring cluster diameters with an accuracy of $\delta\Phi=0.05$ nm. Figure 2 shows that $N(\Phi)/N$ is rather sharp and symmetrical with respect to Φ. The data can be fitted by a Gaussian distribution function (solid line in Fig. 2), from which we obtain the mean cluster diameter $\Phi=3.93$ nm with standard deviation $\sigma_\Phi=\pm 0.6$ nm. In Table I we have collected the data of the mean cluster diameter Φ with standard deviation σ_Φ, the film thickness t, and the metal volume fraction x for all Pd_xC_{1-x} films investigated. As one can see from Table I, the mean cluster diameter Φ is nearly constant, in the range 3 nm $<\Phi<4$ nm.

Figure 3 shows the resistance per square $R_\square$ normalized to the resistance $R_{\square 300}$ at $T=300$ K versus temperature within 1.5 K $<T<300$ K for granular metallic Pd_xC_{1-x} films with $x>0.3$. Data for films with $x<0.3$ are omitted, because they clearly reveal insulating behavior with an exponential temperature dependence.[40]

As one can see from Fig. 3, Pd_xC_{1-x} films with $x>0.35$ reveal a linear, i.e., metallic resistance behavior with $R\propto T$ at elevated temperatures. With decreasing metal volume fraction x, the residual resistance ratio $\Gamma=R_{\square 300}/R_{\square 4.2}$ gradually decreases. Moreover, for films with $x>0.35$ the resistance does not approach a temperature-independent residual "Boltzmann" resistance R_B at low temperatures. Instead, we observe corrections to R_B, with $R_\square(T)$ increasing when the temperature is decreased. This leads to resistance minima at low temperatures. As shown previously, this originates

TABLE I. x is the metal volume fraction, t the film thickness, Φ the mean cluster-diameter, and σ_Φ the standard deviation of Φ.

x	t (nm)	Φ (nm)	$\pm\sigma_\Phi$ (nm)
0.340	21.20	3.93	0.60
0.340	16.81	3.50	1
0.333	27.00	3.02	0.58
0.330	10.60	3.50	1
0.320	28.10	2.82	0.40
0.315	21.60	3.13	0.57
0.314	6.36	3.10	1
0.310	5.80	3.35	0.65
0.304	27.29	3.94	0.64
0.303	8.90	3.83	0.80

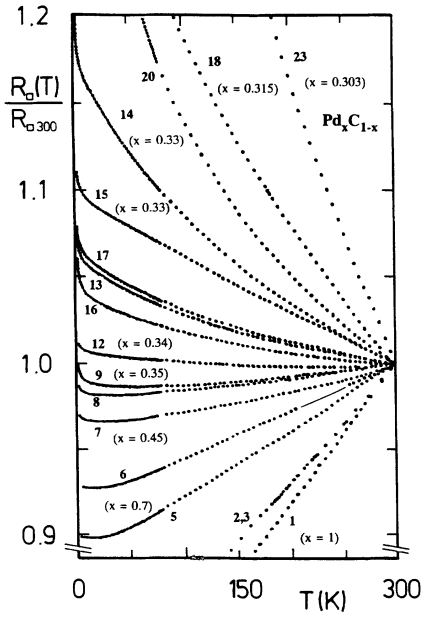

FIG. 3. Resistance per square $R_\square$, normalized to the resistance per square $R_{\square 300}$ at $T=300$ K (see Table II) vs temperature for various metallic Pd_xC_{1-x} films with metal volume fractions within $0.3<x<1$.

from influences of WL and EEI, which increase in magnitude with decreasing metal volume fraction x.[14,17]

Films with $x<0.35$ show a completely different behavior, with $R_\square(T)$ continuously increasing from room temperature down to 1.5 K. From this one could assume that these films are insulating. However, they are indeed *metallic,* because of the following. (i) Structural investigations (TEM) reveal that *all* films contain an infinite cluster network, thus lying definitely above x_p, i.e., on the metallic side. (ii) The temperature dependence of $R_\square$ is neither exponential nor logarithmic. (iii) Instead, we find a power-law behavior $R_\square(T)\propto T^{-\beta}$ with $\beta<1$. We emphasize that such a power-law behavior is typical for disordered *metallic* systems.[41] In Table II we have collected the data for $R_{\square 300}$ and Γ together with the metal volume fraction x for granular Pd_xC_{1-x} films with $0.3<x<1$. Since the conductivity behavior of films with $x>0.35$ has been analyzed earlier,[14,17] in the following we will concentrate on films with $x<0.35$.

In Fig. 4 we have plotted the conductivity $\sigma=(R_\square t)^{-1}$ normalized to the conductivity σ_{100} at $T=100$ K versus $T^{1/2}$ for the films with $0.303\le x\le 0.34$. Values for σ_{100} are given in Table III. As one can see from Fig. 4, the conductivity is proportional to $T^{1/2}$ in a wide range of temperature as indicated by the solid lines. The slope of $\sigma(T)$ increases with decreasing x. At *low* temperatures, however, the $\sigma(T)$ data deviate from the $T^{1/2}$ law toward a stronger temperature dependence. The crossover is indicated by the arrows in Fig. 4. This can be seen in more detail in Fig. 5, where we have plotted $\sigma(T)$ for samples with $x\le 0.33$—here normalized to σ_{30} for convenience—again versus $T^{1/2}$ for $T<30$ K. Values for σ_{30} are also given in Table III. Similar to Fig. 4,

TABLE II. # is a consecutive number x the metal volume fraction, t the film thickness, $R_{\square 300}$ the resistance per square at $T=300$ K, and $\Gamma=R_{\square 300}/R_{\square 4.2}$ the residual resistance ratio.

#	x	t (nm)	$R_{\square 300}$ ($\Omega/\square$)	Γ
1	1	10.00	64.4	1.296
2	0.950	31.45	35.7	1.229
3	0.910	23.41	48.3	1.229
4	0.770	22.59	59.5	1.210
5	0.700	31.54	24.2	1.113
6	0.590	9.81	94.3	1.078
7	0.450	25.70	137.2	1.033
8	0.400	26.60	412.5	1.016
9	0.360	9.32	782.5	1.007
10	0.350	11.20	989.2	1.004
11	0.340	21.20	286.1	0.991
12	0.340	16.81	750.1	0.989
13	0.333	27.00	773.0	0.940
14	0.330	10.60	1806.6	0.847
15	0.330	23.00	547.3	0.907
16	0.324	20.70	1118.5	0.953
17	0.320	28.10	946.4	0.935
18	0.315	21.60	1035.0	0.737
19	0.314	6.36	3975.5	0.773
20	0.130	5.80	6120.0	0.646
21	0.310	23.20	1379.5	0.625
22	0.304	27.29	2006.3	0.617
23	0.303	8.90	5310.0	0.265

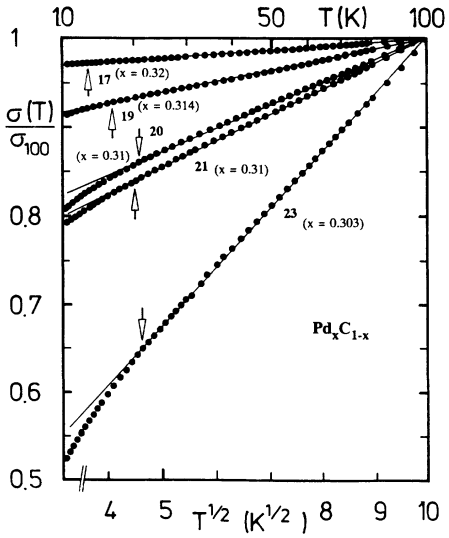

FIG. 4. Macroscopic conductivity $\sigma=(R_\square t)^{-1}$, normalized to the conductivity σ_{100} at $T=100$ K (given in Table III) vs $T^{1/2}$ for typical Pd_xC_{1-x} films within $0.3<x<0.34$. The solid lines are due to a fit from Eq. (3) to the data exhibiting a pronounced $\sigma(T)\propto T^{1/2}$ behavior. The arrows indicate certain temperatures T^* (see Table III), where experimental data deviate from $\sigma(T)\propto T^{1/2}$ at low temperatures.

TABLE III. # is the consecutive sample number, x the metal volume fraction, $\sigma(0)$ the extrapolated conductivity at $T=0$ from a fit of Eq. (3) to the experimental data, Δ a correlation-gap parameter obtained from a fit of Eq. (3) to the experimental data, and T^* the temperature which marks the onset of the deviation from the $\sigma(T) \propto T^{1/2}$ behavior obtained experimentally from $d\sigma/dT$ plots, $T_\delta = \delta/k_B$ is obtained from Eq. (1) using values for Φ from Table I, σ_{100} is the electrical conductivity at $T=100$ K, and σ_{30} is the conductivity at $T=30$ K.

#	x	$\sigma(0)$ $(\Omega\,\mathrm{cm})^{-1}$	Δ (eV)	T^* (K)	T_δ (K)	σ_{00} $(\Omega\,\mathrm{cm})^{-1}$	σ_{30} $(\Omega\,\mathrm{cm})^{-1}$
11	0.340	1632.8	115.50	13	8.2	1647.5	1640.6
12	0.340	786.4	53.30	12	11.6	827.6	791.9
13	0.333	448.4	7.70	13	18	465.8	456.6
14	0.330	437.4	1.42	10	11.6	480.6	456.7
15	0.330	718.2	7.71	13		747.9	731.5
16	0.324	412.0	12.08	15		424.3	418.0
17	0.320	349.9	6.24	13	22	364.6	357.0
18	0.315	322.0	0.59	15	16.2	375.3	343.7
19	0.314	336.0	0.46	17	16.6	381.8	361.2
20	0.310	176.8	0.048	22	13.2	246.3	217.8
21	0.310	177.0	0.027	20		263.9	229.2
22	0.304	105.0	0.054	15	8.1	148.1	128.1
23	0.303	44.5	0.0016	16	8.8	144.6	102.0

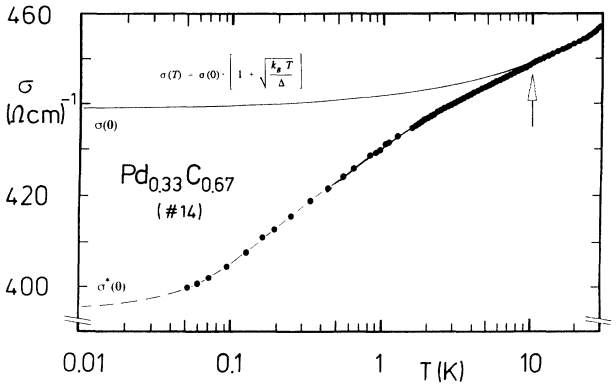

FIG. 6. Semilogarithmic presentation of the macroscopic conductivity σ vs temperature T within 0.05 K $< T <$ 30 K for one of the Pd_xC_{1-x} films (No. 14) shown in Fig. 5 with $x=0.33$. Results for other Pd_xC_{1-x} films are similar or even identical. The solid line likewise represents the $\sigma(T) \propto T^{1/2}$ behavior of the conductivity found to be valid for temperatures $T > T^*$. Note—as is indicated by the dashed line, serving as a guide to the eye—that $\sigma^*(0)$, which is the *true* (extrapolated) conductivity at $T=0$, is smaller compared to $\sigma(0)$, which is the conductivity at $T=0$ extrapolated from the $\sigma(T) \propto T^{1/2}$ behavior, which in turn is expected from Eq. (3) for structurally homogeneous films.

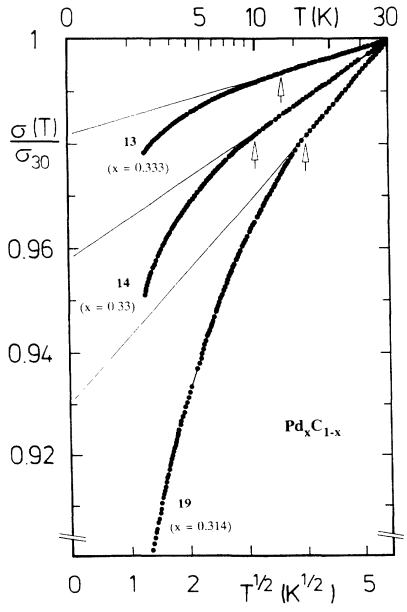

FIG. 5. Macroscopic conductivity $\sigma=(R_\square t)^{-1}$, normalized to the conductivity σ_{30} at $T=30$ K (given in Table III) vs $T^{1/2}$ for typical Pd_xC_{1-x} films within $0.3 < x < 0.34$. The solid lines again represent the fit of Eq. (3) to the experimental data (as shown in Fig. 5), and arrows again mark those certain temperatures T^* where experimental data deviate from $\sigma(T) \propto T^{1/2}$. Note that T^* is nearly identical for all films ranging between roughly 10 K $< T <$ 20 K, independent of both the film thickness t and metal volume fraction x.

below certain temperatures, hereafter denoted T^*, we find deviations from the $T^{1/2}$ law. Values for T^* are given in Table III. The deviations increase in magnitude, when x is decreased. It is remarkable to note that, for all films, T^* lies in a narrow range between 10 and 20 K. T^* is thus independent of both the metal volume fraction x and the thickness t.

In order to investigate the conductivity behavior for $T \to 0$, we have also measured $\sigma(T)$ below 1 K in a $^3He/^4He$ dilution refrigerator. A typical result is given in Fig. 6 for the Pd_xC_{1-x} film with $x=0.33$ (cf. Fig. 5). In Fig. 6 we have chosen a semilogarithmic plot of σ, emphasizing the low-temperature $\sigma(T)$ behavior. As indicated by the dashed line in Fig. 6, which is only a guide to the eye, the conductivity tends toward a finite value $\sigma^*(T=0) \neq 0$ for $T \to 0$. This value is roughly 10% smaller than $\sigma(0)=437.4\ (\Omega\,\mathrm{cm})^{-1}$, which is extrapolated from the high-temperature $\sigma(T) \propto T^{1/2}$ behavior (solid line in Fig. 6). More experiments performed in the mK range, where we checked accurately the sample temperature, reveal a similar behavior for $\sigma(T)$, as shown in Fig. 6 for all Pd_xC_{1-x} films with $0.3 < x < 0.34$,[42] proving the saturation behavior of $\sigma(T)$ for $T \to 0$.

IV. ANALYSIS

For the analysis of $\sigma(T)$ data for our films with $x > x_p$, we make use of a theoretical approach by Castellani *et al.*,[43] dealing with the conductivity behavior of disordered systems in the vicinity of a metal-insulator transition (MIT) taking into account both WL and EEI phenomena. For a 3D system the temperature dependence

of the conductivity is given by[20]

$$\sigma(T)=\sigma(0)\left[1+\left[\frac{k_B T}{\Delta}\right]^{1/2}\right], \quad (3)$$

where $\sigma(0)$ is the conductivity at $T=0$, related to a localization correlation length $\xi \propto 1/\sigma(0)$, which diverges at the MIT. Δ is a correlation gap parameter, which describes the opening of a correlation gap at the Fermi energy E_F with increasing disorder g. Both $\sigma(0)$ and Δ are expected to show *critical* behavior in the vicinity of the MIT with $\sigma(0) \propto |g-g_c|^t$ and $\Delta \propto |g-g_c|^\eta$, both thus going to zero at a certain critical disorder g_c.[43] However, values for t and η are different for various universality classes to which the system may belong.[43]

Disregarding for the moment the experimentally observed deviations from $\sigma(T) \propto T^{1/2}$ for $T<T^*$ (cf. Fig. 5), we have fitted our experimental data to Eq. (3) (cf. solid lines in Figs. 4, 5, and 6) to determine values for $\sigma(0)$ and Δ. Values for the extrapolated conductivity at zero temperature $\sigma(0)$ and the correlation gap parameter Δ are given in Table III, and plotted versus the metal volume fraction x in Figs. 7 and 8, respectively. As one can see from Figs. 7 and 8, both parameters $\sigma(0)$ and Δ diverge for $x \rightarrow x_p=0.3$, thereby characterizing the occurrence of a continuous MIT at the percolation threshold. From plots of $\sigma(0)$ and Δ versus $|1-x/x_p|$ (not shown here), we find $t=1\pm0.3$ and $\eta=3.5\pm0.5$, in rough agreement with theoretical predictions,[43] also corresponding to other experimental results for various disordered systems.[44] However, it is important to note that in our case the MIT obtained in the direct vicinity of the percolation threshold x_p is *not* caused by simple geometrical percolation but by WL and EEI effects, originating from the quantum nature of electronic transport. We emphasize that the extrapolated values of $\sigma(0)$ at $T=0$ in Fig. 7 characterize the occurrence of a continuous MIT at $x=x_p$. The actually measured conductivity below T^* is smaller, and results in different values $\sigma^*(0)$. In the following discussion we will focus on the $\sigma(T)$ behavior at temperatures $T<T^*$, investigating the possible origin of this discrepancy between $\sigma(0)$ and $\sigma^*(0)$.

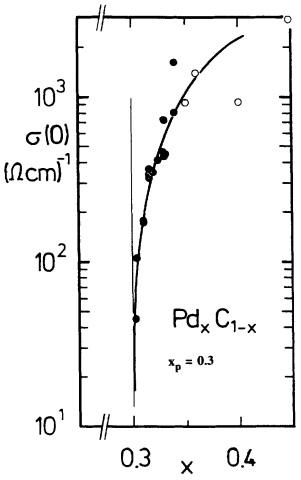

FIG. 7. Semilogarithmic plot of the extrapolated conductivity $\sigma(0)$ at $T=0$, obtained from a fit of Eq. (3) to the experimental data in Figs. 4 and 5, vs the metal volume fraction x for Pd_xC_{1-x} films within $0.3<x<0.34$ (full dots). The open dots correspond to films with $x>0.34$, where $\sigma(0)$ is approximated from $\sigma_{4.2}$ at $T=4.2$ K. Note that $\sigma(0)\rightarrow 0$ for $x\rightarrow 0.3$, which clearly marks the occurrence of a continuous metal-insulator transition right at the percolation threshold at $x_p=0.3$.

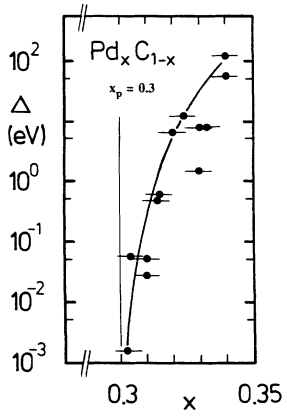

FIG. 8. Semilogarithmic plot of the correlation-gap parameter Δ, obtained from a fit of Eq. (3) to the experimental data in Figs. 4 and 5, vs the metal volume fraction x for Pd_xC_{1-x} films within $0.3<x<0.34$. Again $\Delta\rightarrow 0$ for $x\rightarrow x_p=0.3$ also reveals the occurrence of a continuous metal-insulator transition at the percolation threshold.

V. DISCUSSION

As shown in Figs. 4–6, for $T<T^*$ we observe deviations from $\sigma(T) \propto T^{1/2}$ for all films, which increase in magnitude with decreasing x, i.e., with increasing film inhomogeneity. A detailed investigation of the temperature dependence of $\sigma(T)$ for $T<T^*$ reveals that the data follow neither an exponential nor a logarithmic dependence. Instead, all films show a power-law behavior $\sigma(T) \propto -T^{-\gamma}$ with $\gamma<1$ over nearly two decades in temperature for $0.2\ \text{K} \le T \le 15$ K. The detailed discussion of the temperature dependence of $\sigma(T)$ for $T<T^*$ will be given elsewhere.[45]

The absence of a logarithmic $\sigma(T)$ behavior for $T<T^*$ by no means implies that all films are two-dimensional (2D) with respect to WL and EEI. We checked this in more detail from the analysis of magnetoresistance measurements for $T<T^*$, where we find (a) that all films reveal $\Delta\sigma \propto B^{1/2}$ at high magnetic fields B, as expected for 3D behavior; (b) good agreement between experimental data and theory for 3D WL and EEI at low magnetic fields; and (c) that the experimental results of the magnetoresistance measurements in fields either perpendicular or parallel to the film plane are identical for all films down to the lowest temperature investigated ($T=0.03$ K). From this we conclude that our films can be regarded as being 3D with respect to WL and EEI for $T<T^*$. The respective data along with a comprehensive analysis

of the magnetoresistance measurements will be presented elsewhere.[45]

It is surprising that the T^* values of all granular Pd_xC_{1-x} films with $0.303 \leq x \leq 0.34$ lie in a narrow range $10 < T^* < 20$ K, independent of the film thickness t and the metal volume fraction x (see Table III). Moreover, as TEM investigations reveal, all films are structurally very similar, showing sharp distributions in cluster size around a mean value of $\Phi \approx 3.5 \pm 0.5$ nm (cf. Table I). Since the structure determines the transport behavior, and because of the smallness of Φ, we assume that the electrical properties of our films for $T < T^*$ are modified by quantum size effects (QSE). Indeed, using Eq. (2) with $N(E_F) = 1.463 \times 10^{47}$ $(\mathrm{Jm}^3)^{-1}$ for pure palladium,[46] and Φ as given in Table I, we obtain 0.66 meV $< \delta <$ 1.58 meV, or respectively, for $T_\delta = \delta / k_B$ a critical range 7.7 K $< T_\delta <$ 18.3 K, i.e., almost the same range as found for T^*. Data for T^* and T_δ are given in Table III. Note that respective values for T^* and T_δ are not identical for each sample. A possible reason for this discrepancy is that T^* also depends on the film structure (the particular arrangement of clusters) and not only on the mean cluster diameter as does T_δ. On the other hand, T^* is always remarkably close to T_δ within a few K.

For $T < T^* \approx T_\delta = \delta / k_B$, the onset of energy-level splitting within the clusters thus reduces the number of electrons available for transport. As a consequence, with decreasing temperature those parts of the previously multiply connected cluster network, where QSE take place, are cut off from the network, so that the conductivity decreases more strongly as one would expect from the $T^{1/2}$ dependence. For $T > T^*$ the discrete level splitting is smeared out and $T^{1/2}$ behavior is observed.

On the other hand, why does the conductivity remain finite ($\sigma^*(0)$) for $T \to 0$ and not diverge to zero even in the presence of QSE? This result in turn can only be expected for a network of purely spherical particles, each touching others, with a δ-function-like distribution in size, with the mean diameter corresponding to a certain critical temperature. In our films, however, the size distributions are not δ-function-like. Moreover, "sintering effects" prevent complete spherical clusters, so that in total we observe a smeared out transition. Since in addition, the conductivity takes place within a remaining "backbone" of the network, the conductivity reaches a finite value $\sigma^*(0)$ instead of zero.

Our model is certainly too simple to explain all the details of electronic transport in our granular system, e.g., cluster-charging effects.[3,28] However, the experimental results provide clear evidence for the close correlation of structure and electrical behavior of our films. On this basis, we propose that at low temperatures ($T < T^*$) the electronic transport is influenced by quantum size effects. More future experimental work is certainly desirable to shed more light on the interesting conductivity behavior of granular films in the vicinity of x_p. We hope that our paper will also stimulate further theoretical work in this field.

VI. SUMMARY

We have presented experimental results of detailed investigations of the structural and electrical properties of thin granular Pd_xC_{1-x} films with $0.303 \leq x \leq 0.34$ in the vicinity of the percolation threshold at $x_p = 0.3$. The films consist of an infinite network of small palladium clusters embedded in an insulating carbon matrix. The mean cluster diameters Φ are comparable in magnitude for all films ranging between 3 nm $< \Phi <$ 4 nm. At elevated temperatures all films reveal metallic conductivity behavior exhibiting $\sigma(T) \propto T^{1/2}$, similar to what is expected for 3D films. In close analogy, this is explained as resulting from both electron localization and electron-electron interaction for films in the vicinity of a metal-insulator transition. However, at low temperatures we observe deviations from $\sigma(T) \propto T^{1/2}$, increasing in magnitude with decreasing temperature, where $\sigma(T)$ reaches a finite value $\sigma^*(0) \neq 0$ at $T = 0$, smaller compared to $\sigma(0)$, which in turn is extrapolated from the $\sigma(T) \propto T^{1/2}$ behavior. On the other hand, for all films deviations from $\sigma(T) \propto T^{1/2}$ occur at roughly the same temperature $T^* \approx 15$ K, independent on both the film thickness t and metal volume fraction x. We propose that the deviations in $\sigma(T)$ below T^* result from the structural properties of the films. This is inferred from the experimental finding that T^* is for all films comparable to $T_\delta = [k_B N(E_F) \Phi^3]^{-1}$, which marks the onset of quantum size effects (QSE) with respect to the physical properties of small particle systems. Deviations in $\sigma(T)$ for $T < T^*$ are therefore attributed to the influence of QSE on the conductivity.

ACKNOWLEDGMENTS

We are grateful to Dr. H. Vinzelberg from IFW Dresden for carrying out early conductivity measurements in the mK range for our granular Pd_xC_{1-x} films. This work was partly supported by the Deutsche Forschungsgemeinschaft (DFG), Bonn, Germany, under the Physics of Inorganic Clusters Program. One of us (A.C.) wishes to thank the Alexander von Humboldt Foundation (AvH), Bonn, Germany, for financial support.

*Present address: IBM Research Division, Almaden Research Center 650 Harry Road, San Jose, CA 95120-6099.

[1]For a review see *Physical Phenomena in Granular Materials*, edited by G. D. Cody, T. H. Geballe, and P. Sheng, MRS Symposia Proceedings No. 195 (Materials Research Society, Pittsburgh, 1990).

[2]Ping Sheng, B. Abeles, and Y. Arie, Phys. Rev. Lett. **31**, 44 (1973).

[3]B. Abeles, Ping Sheng, M. D. Coutts, and Y. Arie, Adv. Phys. **24**, 407 (1975).

[4]B. Abeles, H. L. Pinch, and J. I. Gittleman, Phys. Rev. Lett. **35**, 247 (1975).

[5]G. Deutscher, M. Rappaport, and Z. Ovadyahu, Solid State Commun. **28**, 593 (1978).
[6]S. Barzilai, Y. Goldstein, I. Balberg, and J. S. Helman, Phys. Rev. B **23**, 1809 (1981).
[7]N. Savvides, S. P. McAlister, C. M. Hurd, and I. Shiozaki, Solid State Commun. **42**, 143 (1982).
[8]A. D. Inglis, J. R. Dutcher, N. Savvides, S. P. McAlister, and C. M. Hurd, Solid State Commun. **47**, 555 (1983).
[9]S. P. McAlister, A. D. Inglis, and P. M. Kayll, Phys. Rev. B **31**, 5113 (1985).
[10]M. Rohde and H. Micklitz, Phys. Rev. B **38**, 11 895 (1988).
[11]A. Gilabert, M. Skatami, S. Berthier, J. Lafait, and P. Nédellec, Physica A **157**, 223 (1989).
[12]B. Weitzel, A. Schreyer, and H. Micklitz, Europhys. Lett. **12**, 123 (1990); B. Weitzel and H. Micklitz, Phys. Rev. Lett. **66**, 385 (1991).
[13]A. G. Aronov, M. E. Gershenzon, and Yu. E. Zhuravlev, Zh. Eksp. Teor. Fiz. **87**, 971 (1984) [Sov. Phys. JETP. **60**, 554 (1984)].
[14]A. Carl, G. Dumpich, and D. Hallfarth, Phys. Rev. B **39**, 915 (1989).
[15]E. Abrahams, P. W. Anderson, D. C. Licciardello, and T. V. Ramakrishnan, Phys. Rev. Lett. **42**, 673 (1979).
[16]B. L. Al'tshuler and A. G. Aronov, Solid State Commun. **30**, 115 (1979); B. L. Al'tshuler, A. G. Aronov, and P. A. Lee, Phys. Rev. Lett. **44**, 1288 (1980).
[17]A. Carl, G. Dumpich, and D. Hallfarth, Phys. Rev. B **39**, 3015 (1989).
[18]Yoji Koike, Masami Okamura, and Tetsuo Fukase, J. Phys. Soc. Jpn. **54**, 3018 (1985).
[19]G. Bergmann, Phys. Rep. **107**, 1 (1984).
[20]Patrick A. Lee and T. V. Ramakrishnan, Rev. Mod. Phys. **57**, 287 (1985); B. L. Al'tshuler and A. G. Aronov, in *Electron-Electron Interactions In Disordered Systems,* edited by A. L. Efros and M. Pollak (North-Holland, Amsterdam, 1985).
[21]Ch. Van Haesendonck and Y. Bruynseraede, Phys. Rev. B **33**, 1684 (1986).
[22]A. M. Glukhov, N. Ya. Fogel, and A. A. Shablo, Fiz. Tverd. Tela (Leningrad) **28**, 1043 (1986) [Sov. Phys. Solid State **28**, 583 (1986)].
[23]T. Chui, G. Deutscher, P. Lindenfeld, and W. L. McLean, Phys. Rev. B **23**, 6172 (1981).
[24]G. Deutscher, B. Bandyopadhyay, T. Chui, P. Lindenfeld, W. L. McLean, and T. Worthington, Phys. Rev. Lett. **44**, 1150 (1980).
[25]E. Simánek, Solid State Commun. **40**, 1021 (1981).
[26]M. Mostefa and G. Olivier, Solid State Commun. **63**, 219 (1987); J. Phys. C **18**, 93 (1985).
[27]R. Németh and B. Mühlschlegel, Z. Phys. B **70**, 159 (1988).
[28]S. T. Chui, Phys. Rev. B **43**, 14 274 (1991).
[29]O. Entin-Wohlmann, Y. Gefen, and Y. Shapira, J. Phys. C **16**, 1161 (1983).
[30]G. Deutscher, Y. Lévy, and B. Souillard, Europhys. Lett. **4**, 577 (1987).
[31]G. Deutscher, Philos. Mag. B **56**, 725 (1987).
[32]A. Harris Brooks and A. Aharony, Europhys. Lett. **4**, 1355 (1987).
[33]A. L. Efros and B. I. Shklovskii, J. Phys. Solid State C **8**, L49 (1975).
[34]N. Trivedi and N. W. Ashcroft, Phys. Rev. B **38**, 12 298 (1988).
[35]R. Kubo, J. Phys. Soc. Jpn. **17**, 975 (1962); L. P. Gor'kov and G. M. Eliashberg, Zh. Eksp. Teor. Fiz. **48**, 1407 (1965) [Sov. Phys. JETP **21**, 940 (1965)].
[36]R. Denton, B. Mühlschlegel, and D. J. Scalapino, Phys. Rev. Lett. **26**, 707 (1971); Phys. Rev. B **7**, 3589 (1973).
[37]W. P. Halperin, Rev. Mod. Phys. **58**, 533 (1986).
[38]F. A. Shunk, *Constitution of Binary Alloys* (McGraw-Hill, New York, 1969); Ernst Raub and Günter Falkenburg, Z. Metall. **55**, 186 (1964).
[39]Chr. Kuhrt and R. Anton, Thin Solid Films **198**, 301 (1991); R. Huber and P. Ziemann, *ibid.* **174**, 301 (1989).
[40]A. Carl, G. Dumpich, and E. F. Wassermann, Physica B **194-196**, 1101 (1994).
[41]M. A. Howson and B. L. Gallagher, Phys. Rep. **170**, 265 (1988); M. A. Howson, B. J. Hickey, and C. Shearwood, J. Phys. F **16**, L175 (1986); H. H. Boghosian and M. A. Howson, Phys. Rev. B **41**, 7397 (1990); G. Thummes, J. Kötzler, R. Ranganathan, and R. Krishnan, Z. Phys. B **69**, 489 (1988); M. Sanquer, R. Tourbot, B. Boucher, J. M. Broto, and H. Rakoto, J. Non-Crys. Solids **117/118**, 497 (1990).
[42]P. Mikitisin (unpublished).
[43]C. Castellani, C. DiCastro, P. A. Lee, and M. Ma, Phys. Rev. B **30**, 527 (1984); C. DiCastro, in *Anderson Localization,* edited by T. Ando and H. Fukuyama (Springer, Berlin, 1987), p. 96.
[44]R. F. Milligan, T. F. Rosenbaum, R. N. Bhatt, and G. A. Thomas, in *Electron-Electron Interactions in Disordered Systems,* edited by A. L. Efros and M. Pollak (North-Holland, Amsterdam, 1985), p. 231; W. L. McMillan and Jack Mochel, Phys. Rev. Lett. **46**, 556 (1981); Yoseph Imry and Zvi Ovadyahu, *ibid.* **49**, 841 (1982); G. Hertel, D. J. Bishop, E. G. Spencer, J. M. Rowell, and R. C. Dynes, *ibid.* **50**, 743 (1983); M. Gijs, Y. Bruynseraede, and A. Gilabert, Solid State Commun. **57**, 141 (1986).
[45]A. Carl, G. Dumpich, and E. F. Wassermann (unpublished).
[46]M. Gijs, Y. Bruynseraede, and A. Gilabert, Solid State Commun. **57**, 141 (1986).

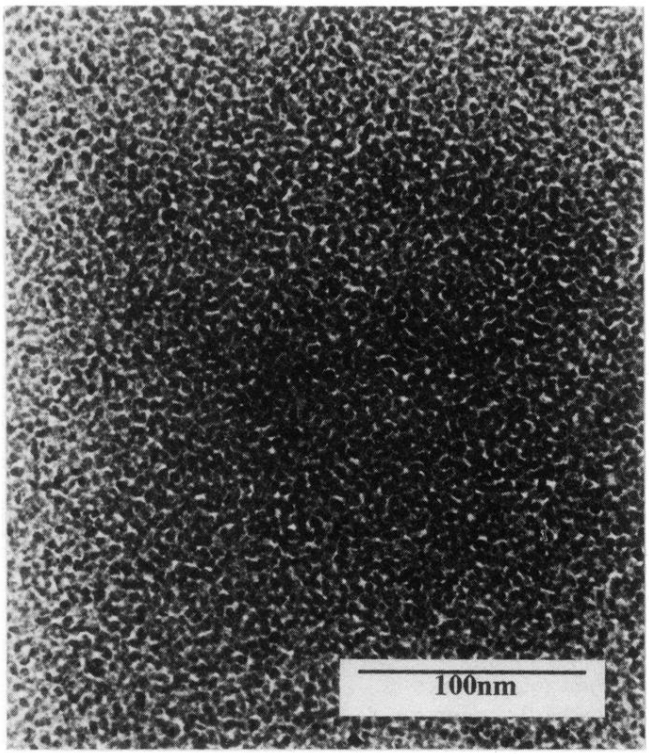

FIG. 1. Electron micrograph of a Pd_xC_{1-x} film with $x=0.34$ and $t=21.2$ nm.